2021 년 8월

석사 학위 논문

A NEW LINKAGE BETWEEN THE METFORMIN DERIVATIVE HL156A INDUCED APOPTOSIS AND AUTOPHAGY IN ORAL SQUAMOUS CELL CARCINOMA

조 선 대 학 교 대 학 원

치 의 생 명 공 학 과

NGUYEN MANH TUONG

A NEW LINKAGE BETWEEN THE METFORMIN DERIVATIVE HL156A INDUCED APOPTOSIS AND AUTOPHAGY IN ORAL SQUAMOUS CELL CARCINOMA

구강 편평 세포 암종에서 메트포르민 유도체 HL156A 유도 세포 사멸과 자가 포식 사이의 새로운 연관성

2021년 8월 27일

조 선 대 학 교 대 학 원

치 의 생 명 공 학 과

NGUYEN MANH TUONG

A NEW LINKAGE BETWEEN THE METFORMIN DERIVATIVE HL156A INDUCED APOPTOSIS AND AUTOPHAGY IN ORAL SQUAMOUS CELL CARCINOMA

지도교수 안 상 건

이 논문을 이학 석사학위신청 논문으로 제출함

2021년 4월

조 선 대 학 교 대 학 원

치 의 생 명 공 학 과

NGUYEN MANH TUONG

NGUYEN MANH TUONG
석사학위논문을 인준함

위원장 조선대학교 교수 최 한 철 인

위 원 조선대학교 교수 지 명 관 인

위 원 조선대학교 교수 안 상 건 인

2021년 5월

조 선 대 학 교 대 학 원

TABLE OF CONTENTS

LIST OF FIGURES

ABBREVIATIONS

AKT	Protein kinase B
AMPK	AMP-activateed protein kinase
ANOVA	Analysis of variance
AO	Acridine Orange
CQ	Chloroquine phosphate
PARP	Poly (ADP-ribose) polymerase
FBS	Fetal bovine serum
mTOR	Mammalian target of rapamycin
MTT	3-(4,5-dimethyl thiazol-2-yl)-2,5-diphenyltetrazolium bromide
OSCC	Oral squamous cell carcinoma
PBS	Phosphate-buffered saline
Dapi	4', 6 diamidino-2-phenylindole
PI	Propidium iodide
RT	Room temperature
SD	Standard deviation
P62	Sequestosome 1
P53	Tumor protein p53
PBST	PBS/0.05% Tween 20

ABSTRACT

A new linkage between the metformin derivative HL156A induced apoptosis and autophagy in oral squamous cell carcinoma

NGUYEN MANH TUONG
Advisor: Prof. Ahn, Sang-gun , PhD
Department of Biodental Engineering,
Graduate School of Chosun University

Metformin, an antidiabetic drug, exerts antitumoral effects in many cancers, including oral squamous cell carcinoma (OSCC). Despite these recent advances, the underlying molecular mechanisms have not been clearly elucidated. Interestingly, our recent studies have reported that metformin derivative HL156A can inhibit the growth of different oral cancer cells. In this study, we examined the antiproliferative role and mechanism of action of HL156A in oral cancer cells. Using MTT and colony formation assay, we found that HL156A has an antiproliferative effect in oral cancer cells that occurred in a concentration-dependent manner. Flow cytometry was used to analyze cell cycle and apoptosis. Exposure to HL156A induced cell cycle arrest in G2/M phase and increased cell apoptosis, which were associated with increased caspase3/PARP activity. On the other hand, HL156A also induced autophagy as demonstrated by acridine orange, autophagic vacuoles staining, and by quantification of the autolysosome-associated LC3 proteins. Interestingly, inhibition of autophagy by autophagy inhibitor chloroquine (CQ) increased the extent of apoptosis, and promoted the antiproliferative

effect of HL156A in oral cancer cells, suggesting that autophagy inhibits HL156A-induced apoptosis. The relevance of these observations was confirmed in vivo system, as we showed that co-treatment with HL156A and CQ treatment strongly inhibited the tumor growth in oral cancer cell xenograft mice. These results showed that HL156A has an antiproliferative effect associated with cell cycle arrest and apoptosis, while is induced autophagy for cell protecting. Taken together, we proved a novel mechanistic insight into antiproliferative effect of HL156A and its therapeutic approach in oral cancer cells.

Ⅰ. INTRODUCTION

Oral squamous cell carcinoma (OSCC) is a prevalent, aggressive, and malignant type of oral cancer, contributing to 90-95% of oral cancers worldwide[1]. Despite numerous improvements in the well-known OSCC therapy, including radiotherapy, chemotherapy and surgery, the 5-year overall survival rate of OSCC is still stagnant at less than 50%. The recurrence rate of OSCC still remaining high[1-3]. Under the demand of novel and effective treatment for OSCC, an abundant amount of targeted therapeutic drugs for OSCC were developed through immeasurable drug discovery and drug repurposing studies.

Metformin, a biguanide-based drug that used to be prescribed for diabetes patients, was studied exhaustively for its anti-cancer effect[4-6]. The anti-cancer effects of metformin are associated with direct and indirect effects of the drug on the host. In terms of the indirect effect of metformin on the host, metformin suppresses cancer development by inhibiting glucose production in the liver[4,5,7]. The direct effect of metformin, on the other hand, is metformin processes by targeting multiple events and pathways such as cell cycle, angiogenesis, glucose metabolism, inflammation, and mammalian target rapamycin (mTOR) and differentiation[4,6,8]. The anti-cancer effect of metformin is mainly mediated through activation of AMPK and inhibition mTOR, which requires the cell membrane transporter OCT1 to uptake in tissue[5,8,9]. However, metformin has an innate limitation due to its natural hydrophilic structure that prevents rapid and passive diffusion through cell membrane, leading to high drug dosage requirements to exhibit its anti-cancer effect (up to 20 mM)[4].

HL156A is a novel derivative of metformin and exhibits superior anti-cancer effect, highlighted by the significant lower concentration required to inhibit tumor progression and cancer cell proliferation[12]. HL156A is a more potent AMPK activator than metformin, and also displayed anti-oxidant effects and showed noticeable anti-cancer effect against drug-resistance cancers cell line[10-14]. Remarkably, our previous studies shown that HL156A inhibited the progression of oral squamous cell carcinoma by alleviating activation of PI3K/AKT/mTOR signaling; HL156A also suppressed multi-drug resistance cancer cell line by inhibiting of MDR1-mediated efflux. Moreover, HL156A was reported with a protective effect on peritoneal fibrosis by suppressed epithelia-mesenchymal transition (EMT), growth factor-β1, and Smad3 pathway. Interestingly, in animal models of glioblastoma, the combination of HL156A and temozolomide suppressed the proliferation and improved survival of cancer stem cells. Recently, a phase I clinical trial was completed to evaluate the impact of HL156A (also known as IM156) in patients with solid tumor[17]. Despite numerous studies investigating the mechanism of effect of HL156A on cancer cell, the molecular mechanism of HL156A was not fully understood[10,13,15]. Since HL156A was developed from metformin, and there are several reports showed that metformin can regulate the autophagy process in multiple cancer cell lines, we came up with a hypothesis that whether HL156A exhibits the similar effect in oral cancer cells? This study was designed to answer that question[6,16,17].

This study illustrated that HL156A, while showing a significant anti-cancer effect, also inducing autophagy in OSCC cell lines YD-15, YD-10B and YD-8. Inhibition of autophagy in vitro and in vivo boosts the anti-cancer effect of HL156A, demonstrated by higher population of apoptotic cells, greater tumor growth suppression, and further inhibition of colony formation. These

results may provide a new approach to the therapeutic potential of HL156A against cancer.

II. MATERIALS AND METHODS

2.1 Cell cultures and reagents

Three different human oral squamous cell carcinoma cell lines (YD-15, YD-10B, YD-8) were purchased from the Korea Cell Line Bank (KCLB, Seoul, Korea). These cell lines were cultured in RPMI-1640 medium (Welgene Inc., Gyeongsanbuk-do, Korea) containing 10% fetal bovine serum (FBS), 100 μg/ml streptomycin and 100 units/ml penicillin in a incubator, supplied with 5% CO2 humidified atmosphere. HL156A is a derivative of phenyl biguanide that was developed and synthesized by Hanall Biopharma Inc. (Seoul, Korea). Detailed information about HL156A's structure and synthesis process was described in a previous study. YD10B and YD-15 were selected for further study because they exhibit higher sensitivity with HL156A treatment.

2.2 Cell proliferation assay

MTT assay was used to measure to analyze cell proliferation. Cells were seeded into 24-well plates at the concentration of 2.5 x 10^4 cells/ well, 24 hours prior drug treatment. On the next day, HL156A was treated in a broad range from 0 to 50 μM for 24h and 48 h. After incubation, cells were washed with PBS and the MTT solution (5 mg/ml in PBS) was added to each well. The MTT solution was removed after 3 hours of incubation in cell culture incubator. Then the insoluble formazan was dissolved in an acidified isopropanol (0.04 mol/L HCl in isopropanol) and then absorbance of the final solution was measured at 540 nm by a DTX 880 Multimode Detector (Beckman Coulter, Brea, CA, USA).

2.3 Clonogenic assay

Cells were pre-treated with different concentrations of HL156A for 24 hours prior harvesting and seeding into a 6-well plate with the density of 500 cells per well. Cells were then incubated for seven days in an incubator for colony development. The colonies were fixed with neutral formalin 10% for 20 min at room temperature and were then stained with 0.05% crystal violet for 30 min. Then the cell colonies were imaged and counting under an IX2-SLP inverted microscope (Olympus, Japan).

2.4 Cell cycle assay and cell apoptosis assay

For apoptosis analysis, cells were harvested and then suspended in RPMI-1640 medium to achieve the final cell concentrations of 5 x 10^5 cells/mL. 100 µL cell suspension were mixed with 100 µL of the Muse Annexin V & Dead Cell Reagent, then incubating for 20 minutes at room temperature, before the cell content were analyzed by Guava Muse Cell Analyzer (Luminexcorp, USA). For cell cycle analysis, Cell was incubated with PI for 15 min at room temperature (RT) in a binding buffer containing saturated concentrations of Annexin V-FITC and PI. After incubation, cells suspension was analyzed in an Attune NxT Flow Cytometer (Waltham, Ma, USA).

2.5 Western blot analysis

Cell were collected by trypsinized and lysised using RIPA buffer containing a protease inhibitor cocktail (1 µg/mL) and phosphatase inhibitor (1 µg/ml). 15 µg of lysates cell were loaded to different concentration SDS-PAGE and transferred to PVDF membrane (Millipore, Burlington, USA). Membrane were blocked with 5% skim milk for 1 hour and incubated with the primary antibodies for at least 4 hours. Antibodies against caspase-3 (sc7148), P53 (sc 126), P62 (sc 28359), p-mTOR (sc 101738) were purchased from Santa Cruz

Biotechnology (Santa Cruz, CA, USA). The antibody against PARP-1 (13371-1-AP) was purchased from Proteintech (Chicago, US). The antibody against LC3B (3868S), AKT (9272S), p-AKT (4060S), Vimentin (5741s), Claudin-1 (13255s) β-Catenin (8480s), Slug (9585s), E-Cadherin (3195s), and the HRP-conjugated secondary antibody were purchased from Cell Signaling Technology (Beverly, MA, USA). After three times washed, the membranes were then incubated with the corresponding secondary antibodies for 1 hour (dilution ratio depended on single antibody). Protein signals were detected and imaged by a Luminescent image analyzer system (LAS-1000; Fujifilm, Tokyo, Japan).

2.6 Caspase 3/7 activity assay

Caspase-3 and Caspase-7 activities were assessed using a Caspase-Glo® 3/7 Assay System (Promega, Madison, Wisconsin, USA) according to the manufacturer's protocol. Briefly, the cells were exposed to different concentrations of HL156A for 24 hours in 96-well white-walled plate. Adding 200 μL of Caspase-Glo® 3/7 reagent to each well and mixing contents of wells using a plate shaker at 300-500 rpm for 30 seconds, then incubating for 1 hour at room temperature. Caspase activity was determined by measuring the luminescence.

2.7. Wound healing assay

Cells were seeded with confluent 2 x 10^5 cells per well into 6-well plate. On the next day, cells were scrapped by a pipet tip, creating an approximately 2 mm scratch on the cell monolayer. Cells were then treated with or without HL156A. Pictures of the scratch were taken at the initial moment, then 12h and 24h by Olympus IX2-SLP inverted microscope (Olympus) at ×100 magnification, to compare the distance of the scratched area.

2.8 Transwell Migration Assay

A modified version of two-chamber migration assay was conducted to determine the cell migration rate. Cells were seeded and treated with or without HL156A for 24 hours, before harvested and suspended in 200 μL serum -free medium. Approximately 2 x 10^5 cells were seeded into the top layer of each upper chamber, and 600 μL complete medium were added in the bottom counterpart. After that, cells were incubated for 24h. Subsequently, the upper chamber was washed twice with PBS to remove the non-attach cells, then the cells were fixed and stained by 0.05% crystal violet solution in 20% methanol for 15 mins at the room temperature. The picture of the migrated cell was taken under IX2-SLP inverted microscope (Olympus, Japan). Finally, the fixed cells were dissolved in 10% acetic acid then the migration rate was quantified colometrically by measuring the optical density value of the solution at 595 nm.

2.9 Immunocytochemistry staining

The intracellular localization of LC3B was detected by immunocytochemistry. Following 24h treatment of HL156A, cells were fixed with neutral formalin 10% for 20 minutes, then permeabilized by the mixture of PBS/1% BSA/0.2% Triton X-100 for 15 min at the room temperature. After that the samples were incubated overnight with LC3B primary antibody (3868S). On the next day, samples were washed by PBS/0.05% Tween 20 (PBST) three times prior incubation with secondary antibodies for 1 h at 37 ° C. Then the samples were washed with PBST three times and then incubated with 4′ ,6-diamidino-2-phenylindole (DAPI) for 10 minutes to stain the nucleic. Images were then obtained using an Olympus IX71 Microscope and HK basic software.

2.10 Acridine orange (AO) staining

To detect whether autophagy was induced in these cells exposed to the HL156A, Acridine Orange, a specific marker for autophagic, was employed to stain for formation of acidic vesicular organelles. Briefly, roughly 2 × 10^5 cells were seeded into a 6-well plate for 24 h before treated with of HL156A for 24 h. Then, cells were stained with 0.1 μM AO (Sigma, USA) in fresh RPMI-1640 and then left it for 30 minutes at 37 ° C, avoiding the light. After three times washing with PBS, the cells were rinsed with PBS then direct images were observed and taken through fluorescence microscope IX71 (Olympus, Japan). Additionally, the number of AO positive cell were detected by flow cytometry (Waltham, Ma, USA) at 360 nm excitation, 530 nm emission.

2.11 Monodansylcadaverine (MDC) staining

Monodansylcadaverine (MDC), a specific marker of autophagic vacuoles, was used to stain autophagosomes. Briefly, roughly 2 × 10^5 cells were seeded into a 6-well plate for 24 h before treated with of HL156A for 24 h. The cells were then stained with 0.05 mM MDC (Sigma, USA) in fresh RPMI-1640, and then left for 30 min at 37 ° C, avoiding the light. Afterward, the cells were washed three times with PBS, then direct images were observed and taken through fluorescence microscope IX71 (Olympus, Japan).

2.12 Animal experiments

Total 32 were used in animal experiments. Approximately 2 × 10^7 YD-15 or YD-10B cells, diluted in PBS, were injected subcutaneously into the right flank of four-week-old BALB/c nude mice. After three days, mice were treated with either PBS, 30 mg/kg Chloroquine, 30 mg/kg HL156A or combination of both Chloroquine and HL156A for every two days, through IP injection. The tumor size was also measured every two days, and the average tumor volume

was calculated using the equation: volume = (L x W2)/2. Mice were killed on day 11, and the tumor was harvested and analyzed through HE staining.

2.13 Statistical analysis

All experiments were performed with the data obtained from three independent experiments. The data are represented as the mean ± standard deviation (S.D). The Student's t-test and one-way analysis of variance (ANOVA) were implemented to calculate the statistical difference between the control and the experimental group. P-value <0.05 was considered statistically significant.

III. RESULTS

3.1 HL156A inhibits oral cancer proliferation and mobility.

3.1.1 HL156A inhibits oral cancer development

MTT assay was conducted to evaluate the effectiveness of HL156A on YD-15 and YD-10B oral cancer cells. In both time and dose-dependent manner, HL156A significantly inhibit the cell proliferation rates of these two cell lines, with the half-maximal inhibitory concentration (IC50) of HL156A against them is approximately 35 μM (Figure 1A, 1B).

To further confirm the inhibitory effect of HL156A, we performed the clonogenic assay. In figure 1C and 1D, the number and the size of colonies in both YD-15 and YD10B were significantly reduced at the dose of 40 μM HL165A. At the concentration of 60 μM, HL156A completely inhibits the colony formation of both these cell lines.

3.1.2 HL156A inhibits cell mobility

The wound healing assay and transwell migration were conducted to evaluate the impact of HL156A to the migration ability of YD-15 and YD-10B cell lines. After scratching, both of them were exposed with 40 μM HL156A for 24 hours. As demonstrated in Figure 1E, treatment with HL156A reduced the wound closure rate remarkably. Additionally, the migration rate of YD-10B and YD-15, after treated with HL156A, also reduced significantly, according to the in vitro trans-well cell migration assay illustrated in Figure 1F and 1G. These figures shown that exposing oral cancer cells to 40 μM HL156A reduced the migration rate by approximately 50%.

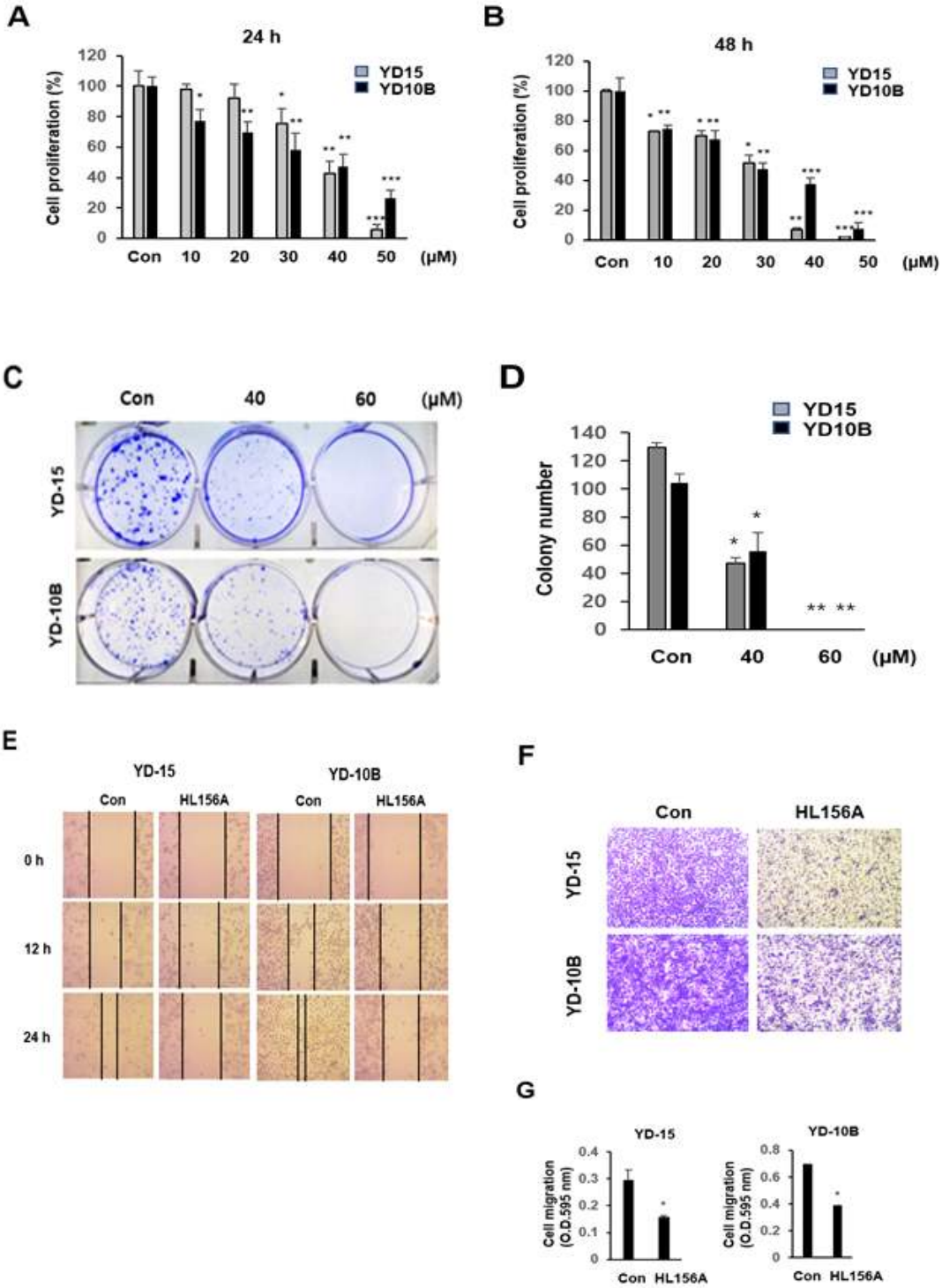

Figure 1. Effects of HL156A on cell proliferation, migration and invasion of human oral cancer cells. (A-B) YD10B and YD15 cells were treated with HL156A (10 to 50 μM) for 24 hour or 48 hours. Cell proliferation was determined using the MTT assay. (C) Results of colony formation assay was assessed 7 days after HL156A treatment at the indicated concentrations, and cells were stained with crystal violet at the end of the experiment. Images were taken with an inverted microscope at x40 magnification. (D) The number of colonies in each plate was graphed. Values are presented as the mean±SD. *p<0.05 and **p<0.01. Data were compared by ANOVA with Bonferroni's multiple comparisons test. (E) A wound healing assay showed the closure rates of YD15 and YD10B cells treated with HL156A 40 μM for 12 hour and 24 hours. (F) The effect of 24h treatment of HL156A on cell migration. (G) Quantitative value of the migration rate was graphed. *p < 0.05, **p < 0.01. Data are expressed as the mean ± SD. Data were compared by Student's t-test and ANOVA with Bonferroni's multiple comparisons test for determination the statistical difference between more than one group.

3.2 HL156A increases G2/M cell cycle arrest and cell apoptosis

Our previous paper already demonstrated effect of HL156A on Fadu cell, another oral cancer cells line, including the cell cycle arrest and cell apoptosis induction. Therefore, we continue to analyze the influence of HL156A to cell cycle progression and cell viability of YD15 and YD10B by flow cytometry, and the result in figure 2A shown that treatment of HL156A induced the cell cycle arrest at phase G2/M. In particular, the percentage of the G2/M population increased from 2.0% to 6.3% in YD-15 cell lines, and from 4.4% to 8.5% in the YD10B cell lines.

Through flow cytometry, we also found verify that HL156A can induced the

cell apoptosis in the oral cancer. Figure 2B illustrated that HL156A treatment resulted in an increase of the apoptotic cells population, from 5% to 18.9% in YD-15 and from 5.6% to 28% in YD-10B cell lines. Consistent with the flow cytometry result, Western blot analysis illustrated that treatment of HL156A in a dose dependent manner reduces the inactive form of caspase-3 and poly (ADP-ribose) polymerase (PARP), two markers of cell apoptosis (Figure 2C). Intracellular activity of Caspase 3/7, two major regulators of apoptosis, increased significantly after treatment of HL156A, as demonstrated in Figure 2D.

HL156A can suppress the AKT/mTOR pathway to decelerate the progression of oral cancer in FaDu cell line, as demonstrated in our previous paper. Through Western Blot, we confirmed that HL156A not only targets the AKT/mTOR pathway, but also inhibits the expression of Sirtuin 1 (SIRT1), a NAD-dependent deacetylase enzyme that involves in numerous cellular progressions, including the Epithelial-mesenchymal transition (EMT), a process that associated with cell migration and cell invasion. Since HL156A treatment can inhibit both SIRT1 expression and cell migration/invasion ability, we decided to investigate the impacts of HL156A treatment toward EMT, to get further understanding about the anti-cancer effect of HL156A.

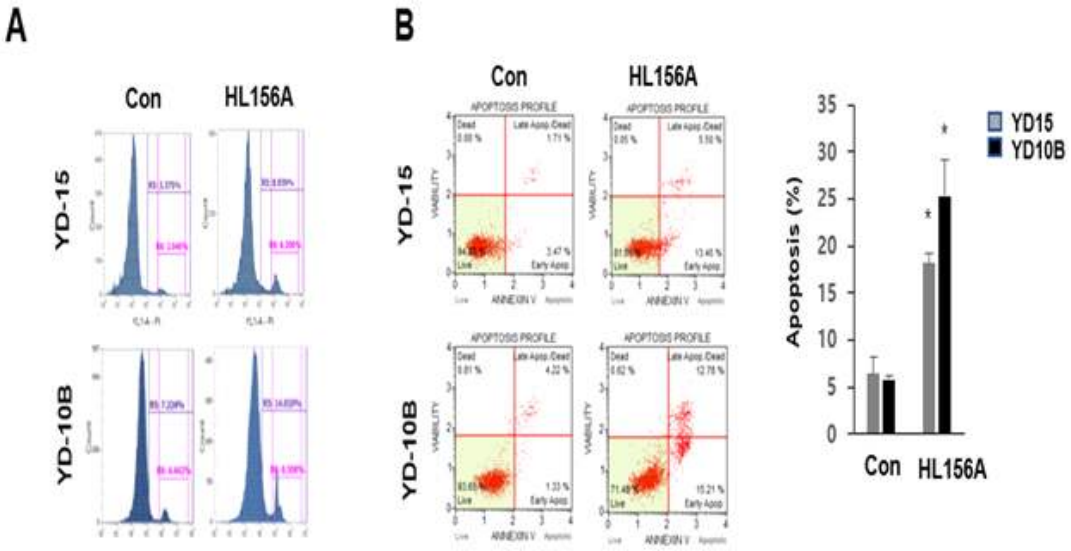

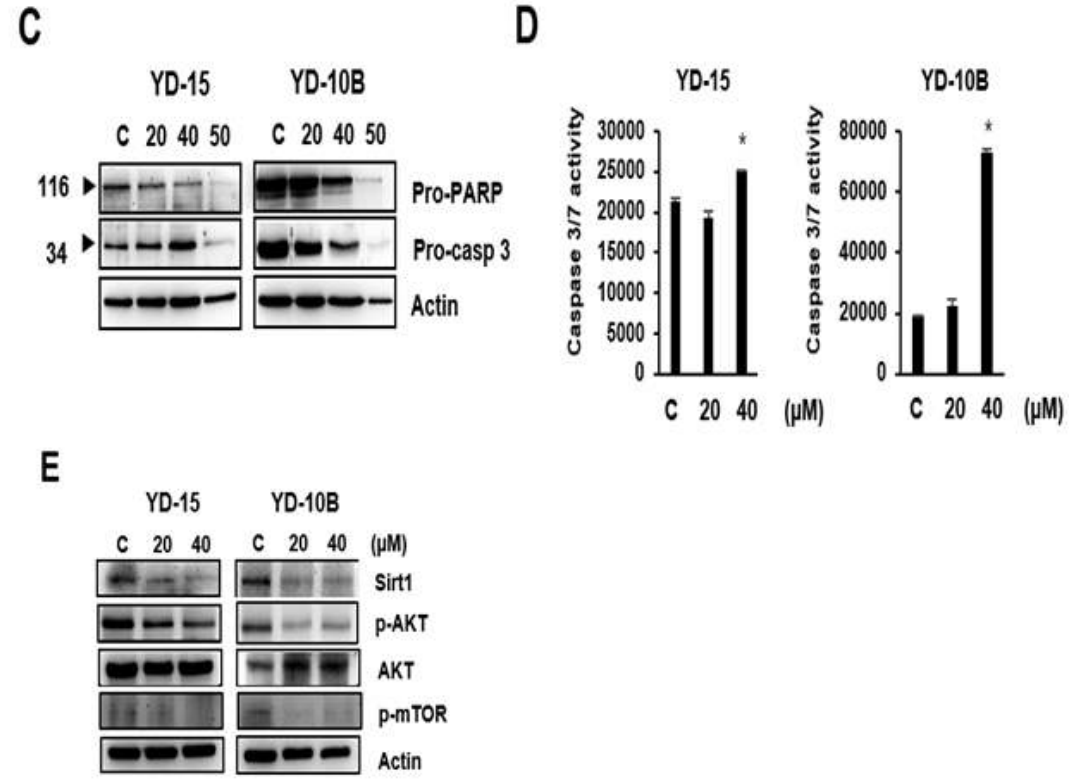

Figure 2. HL156A induces cell cycle arrest and cell apoptotic. (A) YD-15 and YD-10B cells were exposed to 40 μM of HL156A for 24h, and the cell cycle were assessed cytometry after staining with PI (B) The apoptotic cells were evaluated by dual staining with Annexin V/PI and counted by flow cytometry. *p<0.05 and **p<0.01. (C) HL156A reduced inactive form of caspase 3 and PARP. Cells were treated with HL156A for 24h prior examination by Western Blot (D) Quantifying intracellular activity of caspase 3/7 in YD15 and YD10B cells line after 24h of HL156A treatment. (E) HL156A repressed the ATK/mTOR pathway and SIRT1 expression. * $p < 0.05$. Data are expressed as the mean ± SD. Data were compared by ANOVA with Bonferroni's multiple comparisons test for determination the statistical difference between more than one group.

3.3 HL156A can regulates EMT markers

We examined the expression of EMT markers to investigate the influence of HL156A treatment toward EMT. Interestingly, treatment of HL156A at different dose yields different effect on the EMT markers (Figure 3). At the 40 μM (IC50 dosage), majority of mesenchymal and epithelial markers are inhibited. However, in the only YD-15 cell lines, treatment of HL156 at 20 μM induces the expression of epithelial markers(E-cadherin, β-catenin and Claudin), while represses the expression of mesenchymal markers(N-cadherin, Vimentin and Slug) , indicated potential of reversing EMT process of HL156A treatment.

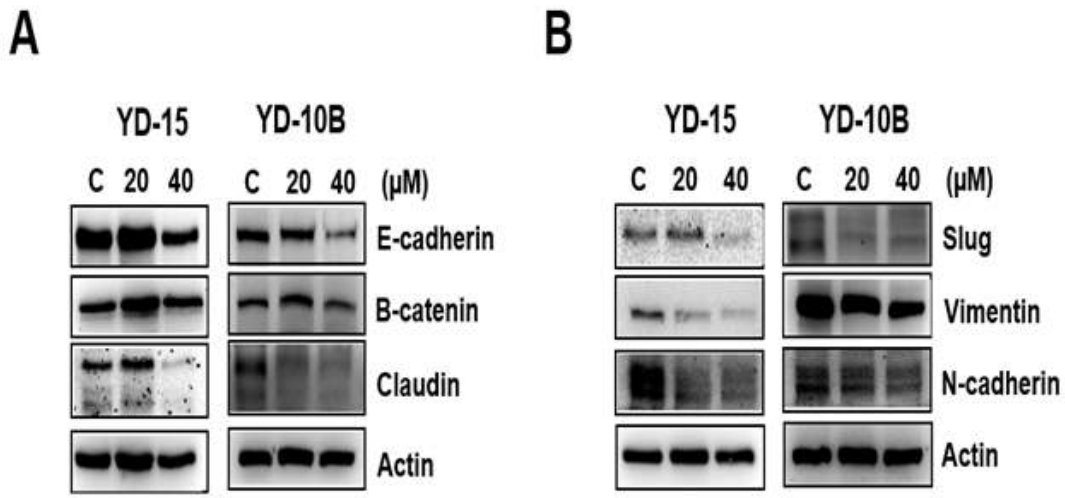

Figure 3. HL156A regulates EMT markers. Analysis of EMT markers expression by Western blot. Cell were treated with HL156A for 24h prior experimented. (A) Epithelial markers. (B). Mesenchymal markers.

3.4 HL156A induces autophagy in the OSCC

It was reported that metformin can induce the autophagy in several type of cancer cell lines[8,9,18]. Since HL156A is a derivative of metformin, we decided to check whether HL156A can trigger autophagy in OSCC. Interestingly, treatment of HL156A induces the expression of LC3B (marker of autophagic flux) while decreases the expression of p62 (marker of autophagosome degradation), as shown in Figure 4A, suggesting that autophagy may be induced. We continued with immunocytochemistry to detect the formation of intracellular LC3B puncta, and the results illustrated a significant increase in LC3B-positive structures (Figure 4B). Finally, we confirmed the HL156-induced autophagy through acridine orange (AO) and mono-dansylcadaverine (MDC) staining, respectively. As demonstrated in Figure 4C and 4D, treatment of HL156A induces the formation of lysosome and autophagic vacuoles, thus verifies that HL156A treatment can induce the autophagy in OSCC.

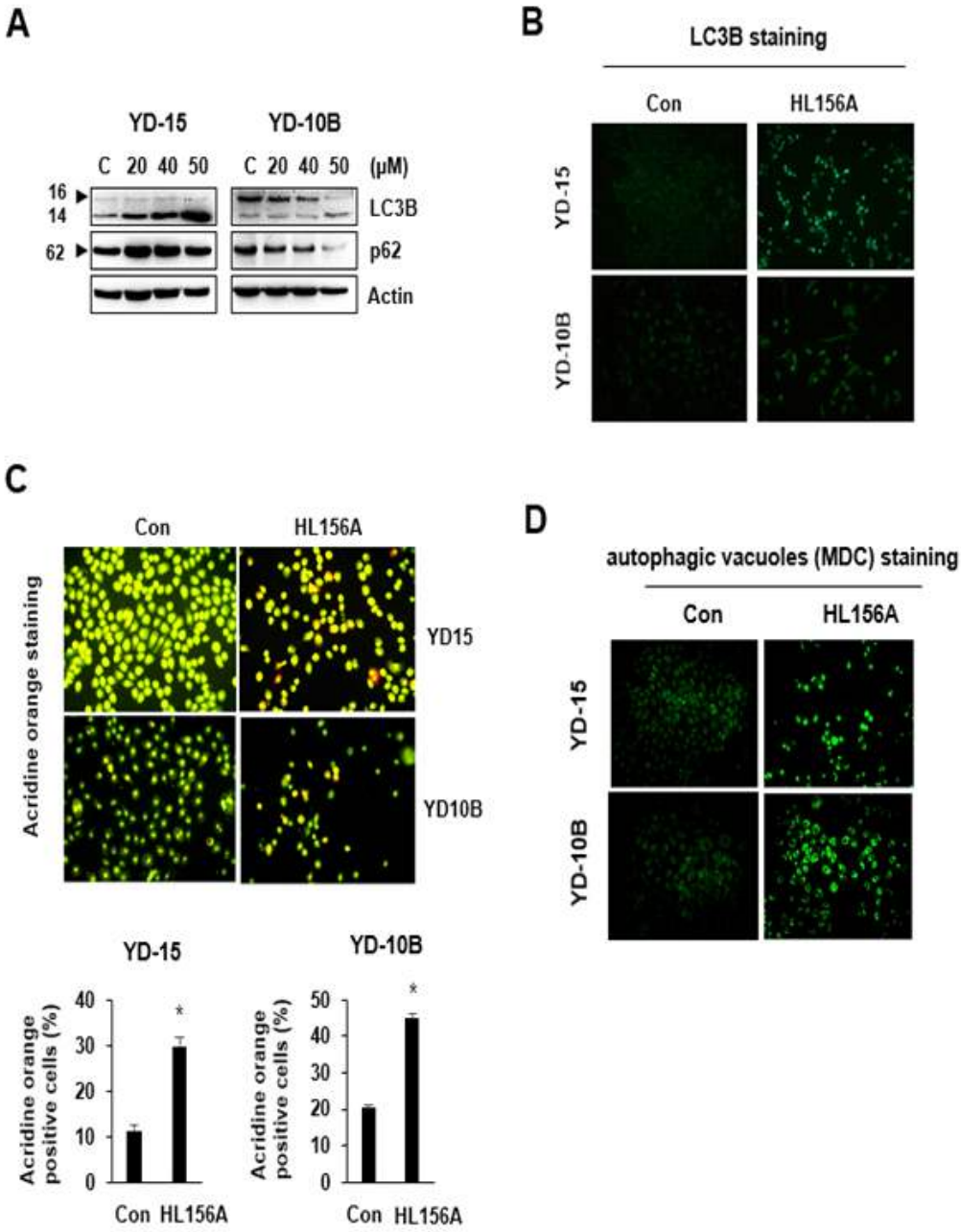

Figure 4. HL156A induces autophagy in OSCC. (A). Analysis of autophagy markers by Western Blot. Cells were treated with different concentrations of HL156A 24h prior experimented. (B). Immunocytochemistry staining were performed on cell treated with our without HL156A 40 μM for 24h. (C) AO staining were applied to evaluate the formation of lysosome in HL156A treated cells. The number of AO-positive cells were counted by flow cytometry. (D) MDC staining were conducted to detect the formation of autophagic vacuoles in HL156A treated cells. Images were taken by fluorescence microscope IX71. * $p < 0.05$. Data are expressed as the mean ± SD. Data were compared by Student's t-test.

3.5 Inhibition of autophagy improves the anti-cancer effect of HL156A in OSCC.

The impact of autophagy in cancer is convoluted and not well understood yet. Autophagy is a double-edged sword, exhibits both pro-survival and pro-death characteristics, depending on numerous conditions, including cancer type, location, progression, and even type of cancer treatment[5,6]. Thus, we decided to investigate the role of autophagy toward the anti-cancer effect of HL156A in OSCC, using autophagy inhibitor Chloroquine (CQ).

MTT assay revealed that a single treatment of CQ does not alter the cell proliferation rate, but a combination of CQ and HL156A significantly reduces the cell viability of YD-15 and YD-10B (Figure 5A-5B). Co-treatment of CQ and HL156A also boosts the cell cycle arrests at phase G2/M, as demonstrated in Figure 5C, especially in YD-15, with an increase from 5.2% to 21.5%. Similarly, the population of apoptotic cells almost doubled in combination samples, compared with single treatment of HL156A, illustrated in Figure 5D and 5E. Western Blot analysis showed that the inactive form of Caspase 3 and PARP, two apoptosis markers, are greatly reduced in the presence of both HL156A and CQ.

Additionally, the clonogenic assay showed that both the number and size of the formed colony are significantly inhibited in HL156A and CQ co-treated samples (Figure 6A). We also evaluate the expression of EMT markers to check whether inhibition of autophagy affects the ability of HL156A to regulate EMT markers. As illustrated in figure 6B, the expression of Vimentin (epithelial marker) and Claudin (mesenchymal marker) are further abrogated in the combination treatment, compare with a single treatment of HL156A. In summary, these data indicated that CQ can synergize with HL156A to boost

its anti-cancer effect in YD-15 and YD-10B oral cancer cells.

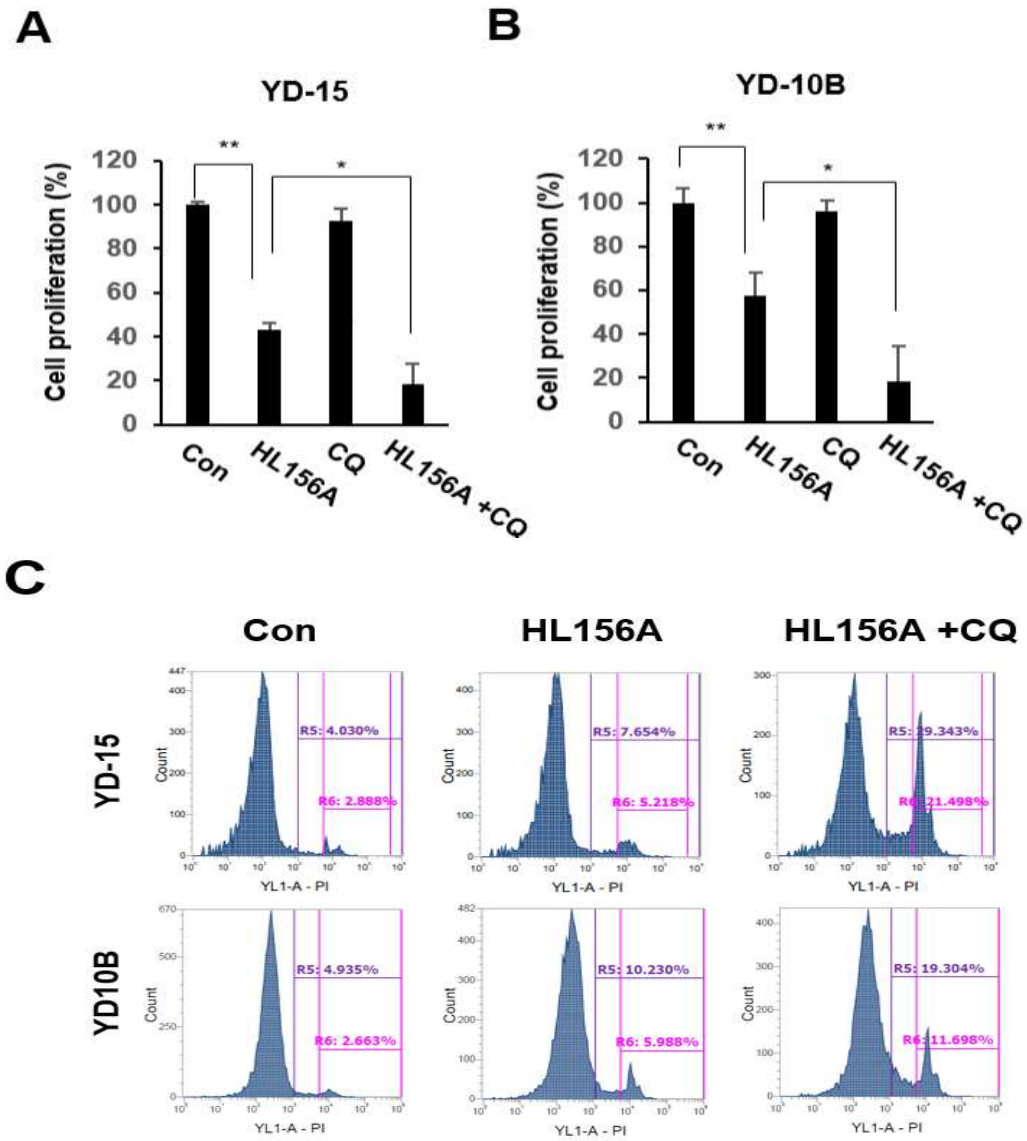

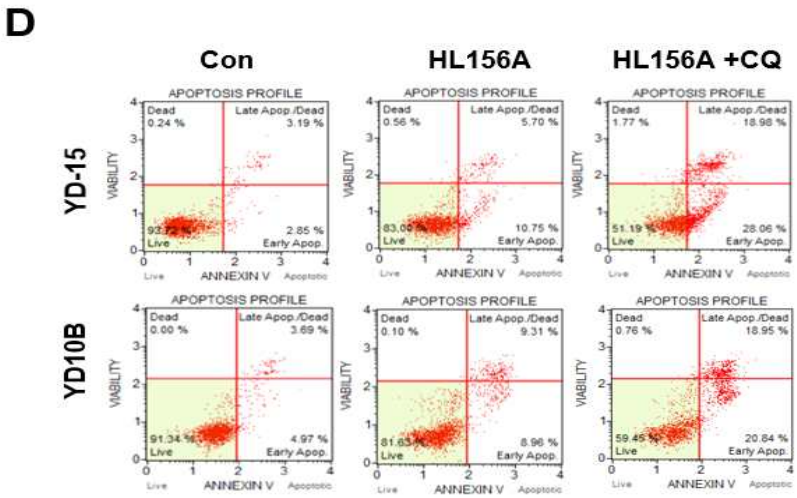

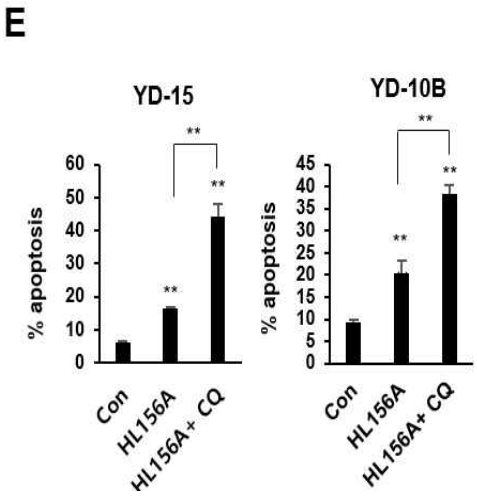

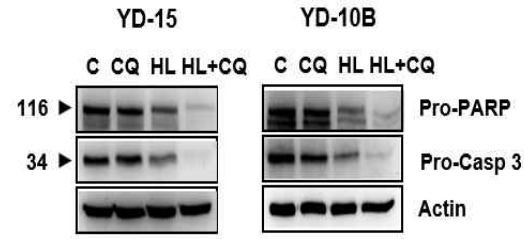

Figure 5. Inhibition of autophagy improves the anti-cancer effect of HL156A in OSCC. Cells were treated with 40 μM of HL156A, 40 μM of CQ, or a combination of both, 24h prior experimented. (A and B). Analysis of cell proliferation by MTT assay. (C) Cell cycle distribution was examined by flow cytometry, showed that a combination of CQ and HL156A greatly induced cell cycle arrest at the G2/M phase. (D and E) Apoptotic cell percentage was assessed by flow cytometry and the percentage of the apoptotic cell were graphed. Co-treatment of CQ and HL156A increase the cell apoptosis significantly (F) Western Blot was conducted to analyze the pro-apoptosis markers in single treated and co-treated samples. * $p < 0.05$, ** $p < 0.01$. Data are expressed as the mean ± SD. Data were compared by ANOVA with Bonferroni's multiple comparisons test.

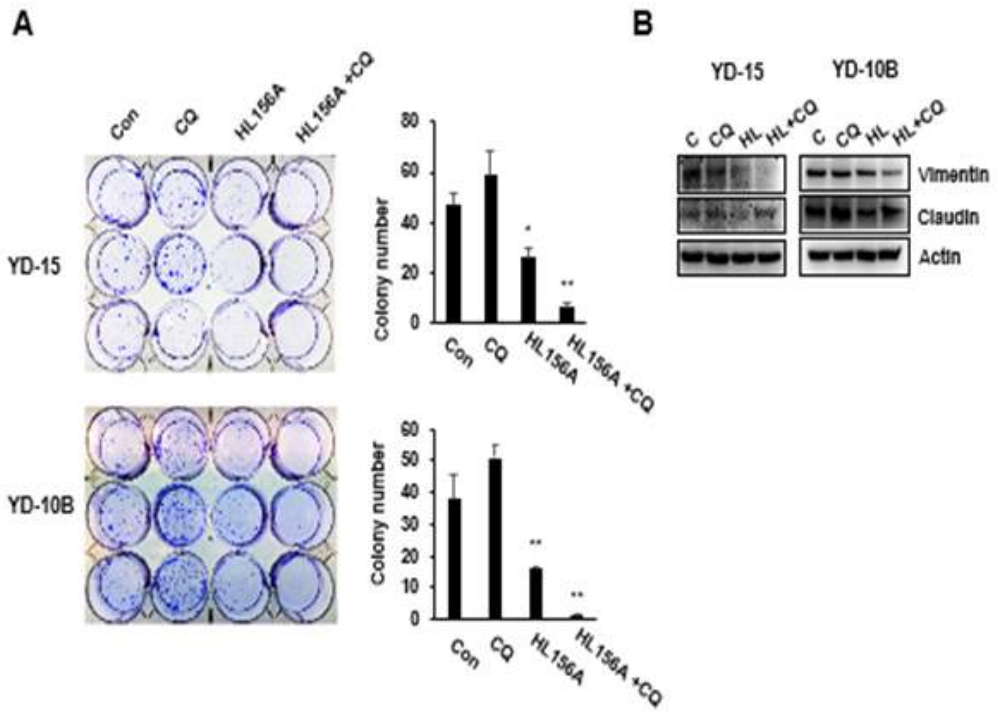

Figure 6. Co-treatment of HL156A and CQ inhibit colony formation and EMT markers. (A) Cells were treated with 40 μM of HL156A, 40 μM of CQ or a combination of both, 24h prior seeding with low density (500 cells/well) and letting colony formation for 7 days. Cell were stained by crystal violet 0.05% then pictures were taken, and the number of colonies were counted and graphed. (B) Western Blot were conducted to analyze the EMT markers in single treated and co-treated samples * $p < 0.05$, ** $p < 0.01$. Data are expressed as the mean ± SD. Data were compared by ANOVA with Bonferroni's multiple comparisons test.

3.6. Chloroquine augments HL156A anti-cancer effect in nude mice model.

To validate the synergy between CQ and HL156A, we conducted in vivo experiments on nude mice model. 4-week-old BALB/c nude mice were selected randomly and 2 x 10^7 cells were injected in the right flank. Detailed information was described in the Material and Method section. As demonstrated in Figure 7A and 7B, combination of HL156A and CQ greatly reduces the tumor volume and tumor weight, up to almost 100% in YD-10B cells, while do not impact the average bodyweight or causing serious side effects, as indicated in figure 7C. The detailed value of tumor volume were graphed in Figure 7D. HE staining were applied to analyze the histological difference between each sample group. Compare with the HL156A treatment group, the combination group has larger percentage of nuclear fragmentation and disruption in the connecting tissue structures.

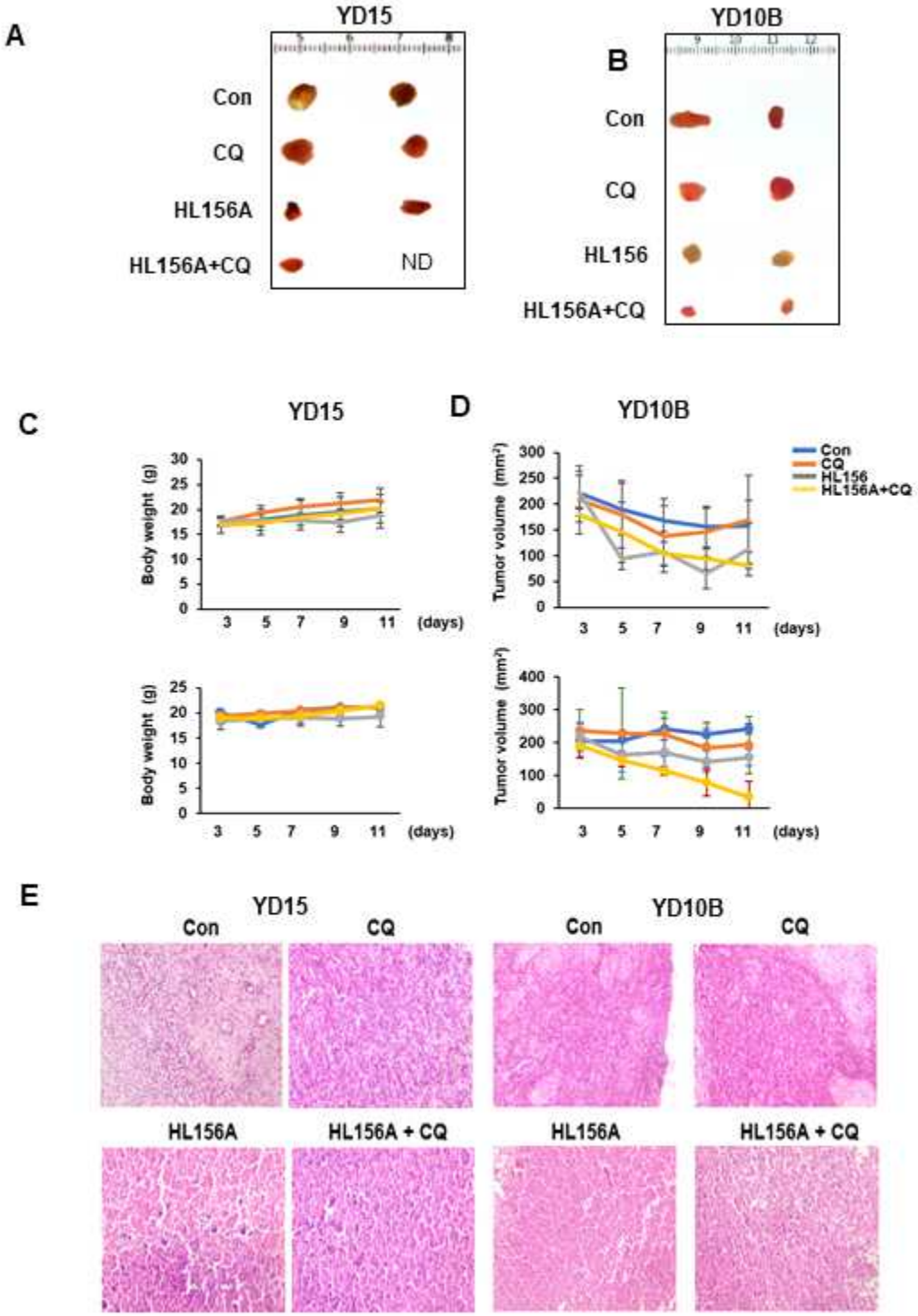

Figure 7. Chloroquine augments HL156A anti-cancer effect in nude mice model. (A and B) Tumors were isolated from mice that were treated Chloroquine, HL156A or combination of both Chloroqine and HL156A after four times injection. (C-D) The tumor size and body weight were also measured every two days. (E) H&E-stained serial sections of the same xenografts are presented.

3.7. Effect of HL156A on YD-8 oral cancer cell line.

The efficacy of drug treatment can be varied on different type of cancer. Our MTT data showed that the YD-8 oral cancer cell lines showed higher resistance toward HL156A treatment, compare with YD-15 and YD-10B (Figure 8A). The IC50 of HL156A against YD-8 cell line is 90 μM, approximately tripled that of YD-10B and YD-15. Despite the high resistance of YD-8 cell line, HL156A still is capable of inhibiting colony formation. Particularly, colony formation was totally inhibited in the HL156A-treated group compare that of control group (Figure 8B). Similar to YD-10B and YD-15, HL156A also induced cell cycle G_2/M phase by increasing three times the population of the G_2/M compare to that of control on YD-8 cell line (Figure 8C). Consistent with previously reported data, treatment of HL156A leads to a reduction in cell migration ability (Figure 8D). Next, the number of cell apoptotic of YD-8 cells which was exposed HL156A was dramatically increased from 7,2 % to 24,9% (Figure 8E). The inducing apoptosis cell ability of HL156A was further confirmed by western bot. The apoptotic markers (pro-PARP and pro-Caspasse 3) observed on the HL156A treated group was greater, compared with corresponding control groups (Figure 8F).

Similar with YD-10B and YD-15, treatment of HL156A on YD-8 also induces the autophagy flux. LC3B expression were upregulated under the effect of HL156A for 24h, confirmed through Western Blot (Figure 9A). The formation of

intracellular LC3B-positive puncta were confirmed by immunofluorescence staining (Figure 9B). We also confirmed an increase in the number of lysosomes and autophagic vacuoles in HL156A-treated samples by AO staining and MDC staining (Figure 9C and 9D). Consistent with our previous findings, HL156A targets both AKT/mTOR pathway and SIRT1 protein (Figure 9E). These data illustrated that the effect of HL156A remained the same in the oral cancers cell line.

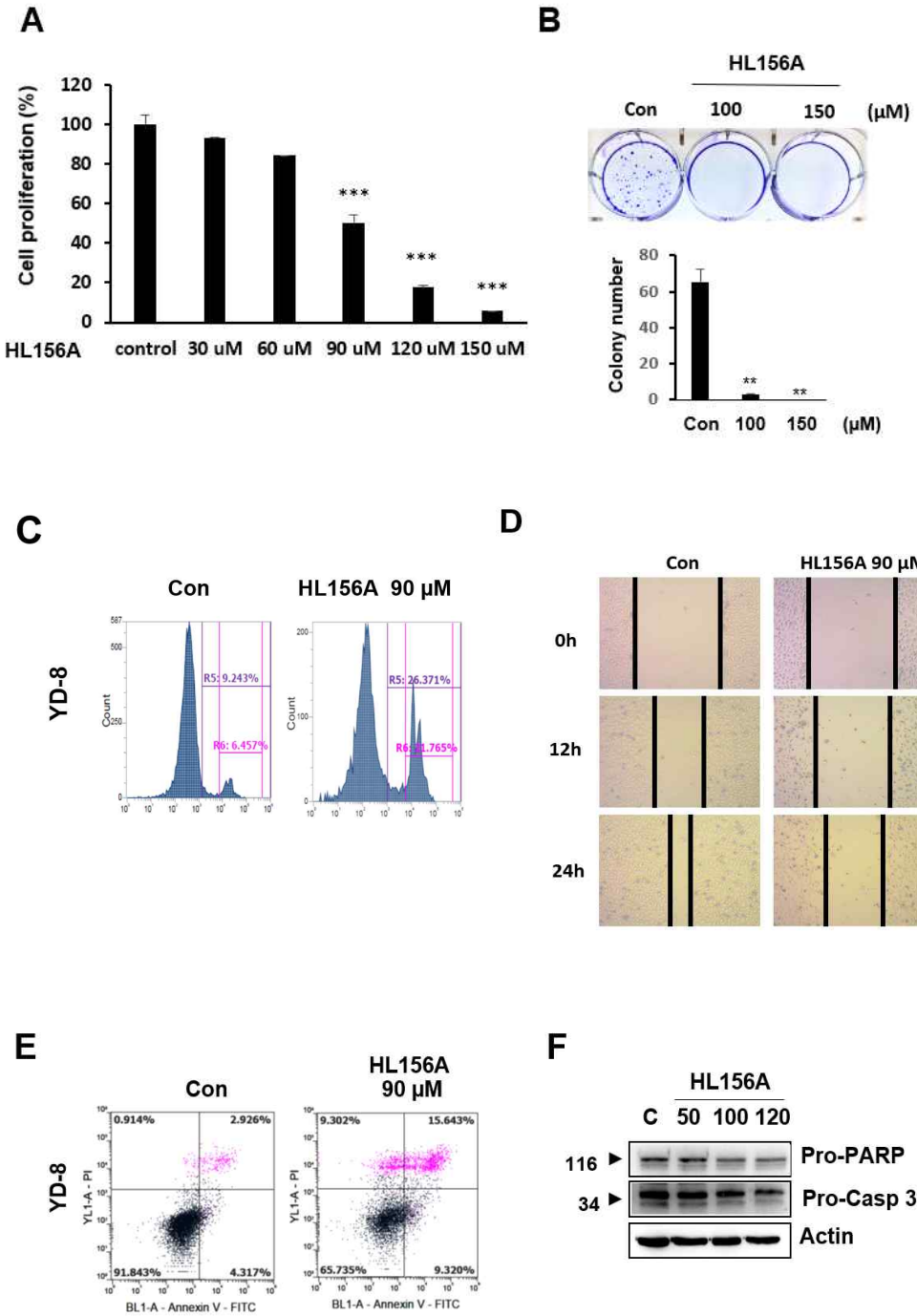

Figure 8. Effects of HL156A on cell proliferation, migration, and invasion of YD-8 oral cancer cell line. (A) YD-8 cells were treated with HL156A (10 to 50 μM) for 24 hours. Cell proliferation was determined using the MTT assay. (B) Results of colony formation assay were assessed 7 days after HL156A treatment at the indicated concentrations, and cells were stained with crystal violet at the end of the experiment. Images were taken with an inverted microscope at x40 magnification and the number of colonies in each plate was graphed. (C) YD-8 cells were exposed to 90 μM of HL156A for 24h, and the cell cycle were assessed cytometry after staining with PI. (D) A wound-healing assay showed the closure rates of YD-8 cells treated with HL156A 90 μM for 12 hours and 24 hours. (E) The apoptotic cells were evaluated by dual staining with Annexin V/PI and counted by flow cytometry. *$p<0.05$ and **$p<0.01$. (F) HL156A reduced inactive forms of caspase 3 and PARP. Cells were treated with HL156A for 24h prior examination by Western Blot.

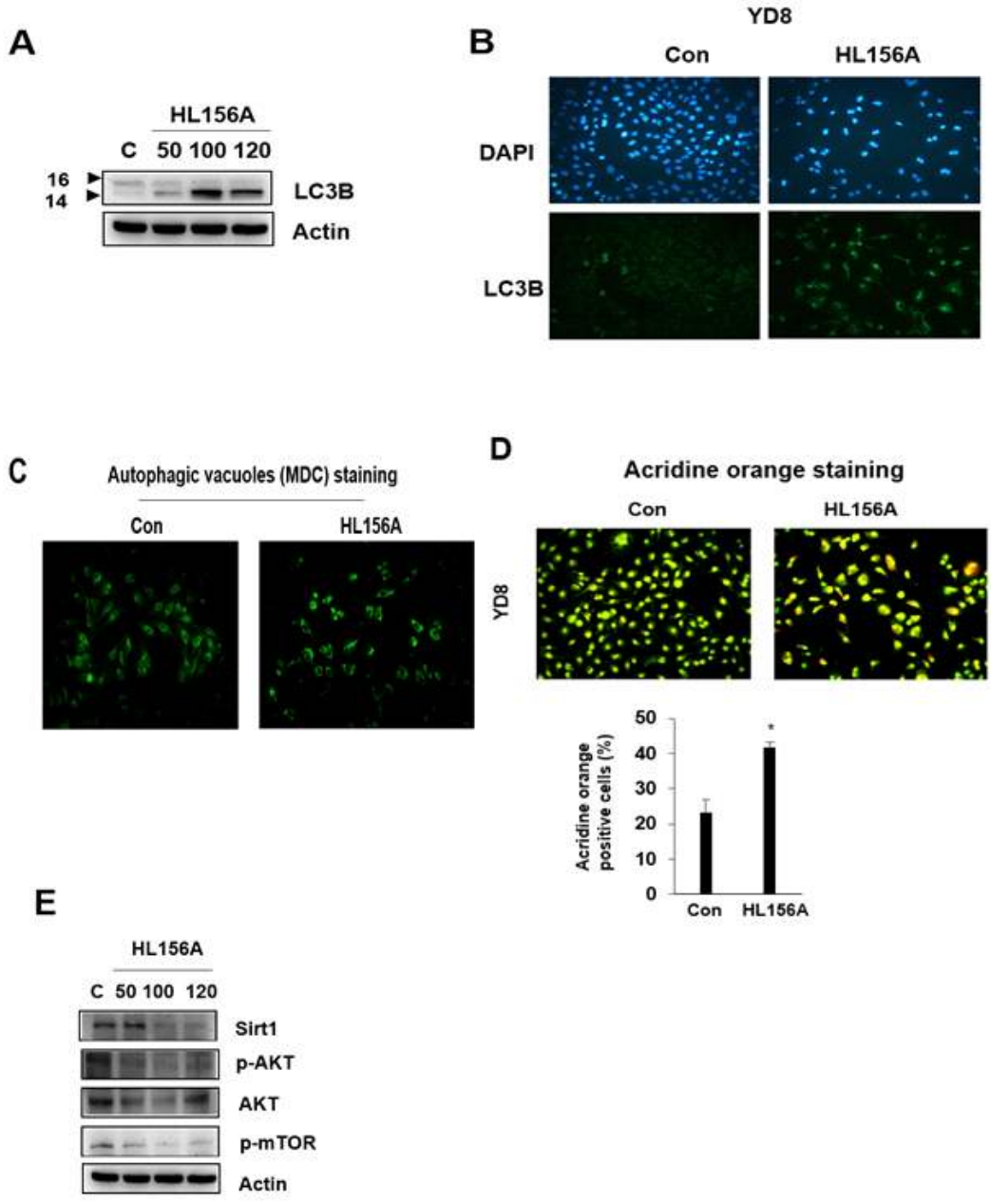

Figure 9. HL156A induces autophagy in YD-8 oral cancer cell line. Analysis of autophagy markers by Western Blot. Cells were treated with different concentrations of HL156A 24h prior experimented. (B). Immunocytochemistry staining were performed on cell treated with our without HL156A for 24h. (C) MDC staining were conducted to detect the formation of autophagic vacuoles in HL156A treated cells. Images were taken by fluorescence microscope IX71. (D) AO staining were applied to evaluate the formation of lysosome in HL156A treated cells. The number of AO-positive cells were counted by flow cytometry. (E) HL156A repressed the ATK/mTOR pathway and SIRT1 expression. * $p < 0.05$. Data are expressed as the mean ± SD. Data were compared by Student's t-test.

IV. DISCUSSION AND CONCLUSION

Recently, metformin has aroused interest in its anti-cancer effects. The impact of it within the inhibition of cancer is related to both direct and indirect effects. The directly anti-cancer effect of metformin in the host inhibits the transcription of crucial gluconeogenesis genes in the liver and glucose uptake in muscle, declining blood glucose, and raising insulin[4,6,8]. The development of cancer requires a fuel-rich environment with a high level of glucose. As a reducing glucose agent, metformin cut off supplies for cancer cells, resulting in suppressing tumor development in the host. Also, metformin is known as an anti-cancer reagent by directly targeting multiple pathways on cancer cells[6]. In cancer metabolism, metformin effects negatively in lipid biosynthesis, glucose metabolism, and protein metabolism. Metformin targets the mitochondria and suppresses complex I, which induces AMPK activation and inhibits mTOR signal; it promotes program cell death signaling pathways such as apoptosis, proptosis, and autophagy[5,8,9,18]. Moreover, the cell cycle of the cancer cell is also repressed by metformin through activation of P53.

HL156A, metformin derivate, is a newly developed drug by Hanall Biopharma Inc. since 2016, and it already shows great potential in cancer treatment, exhibits great antiproliferative effect against multiple types of cancer cells, including glioblastoma, breast cancer, gastric cancer, and oral cancer; as well as typical cancer and drug-resistant cancer[10-13,19]. However, the impact of HL156A on cancer cells is not fully understood, and how much similarity HL156A shares with its precursor, metformin, still unanswered. In our previous study, HL156A was reported that strongly inhibited cell proliferation and suppressed cell cycle in oral cancer cell line and human

multi-drug resistance cancer cells. In this study, we investigated the effect of HL156A in three oral cancer cell lines, including YD-15, YD-10B, and YD-8. Our study illustrated that HL156A induced cell death by activating cell apoptosis through increasing caspase 3/7 activities. On the other hand, HL156A triggers autophagy protection by increasing LC3B and P62 protein expression; It leads to suppress apoptosis induces cell death. Additionally, using Chloroquine which inhibited HL156A-induced autophagy, significantly improve the efficacy of HL156A (Figure 10). Different from its precursor, HL156A inhibits the expression of SIRT1 and probably inhibits the EMT process through SIRT1 signaling. This study provided a novel insight into the molecular mechanism of HL156A toward OSCC, and it could be useful for further clinical application.

Interestingly, we found a noticeable difference between HL156A and its precursor, metformin. Metformin was reported multiple times as a direct activator of SIRT1; however, our data showed that HL156A treatment inhibits SIRT1 expression in all three oral cancer cell lines (Figure 1 and Figure 9)[8,20]. Previously our group demonstrated that pharmacologic inhibition of SIRT1 can suppress cancer cell migration[21]. In the concept of tumor development and tumor metastasis, cells usually gain mobility to migrate and invade through the epithelial-mesenchymal transition (EMT) process. SIRT1, a highly conversed NAD-dependent deacetylases, is involved in diverse cellular activity, including cellular metabolism, cellular homeostasis, cellular apoptosis[22-26]. In cancer, SIRT1 roles are convoluted and usually contradictive, including oral cancer, as was summarized by Islam et al[27]. In the narrow field of EMT, literature reported that SIRT1 regulated EMT in a context-dependent manner, as it was found that SIRT1 can suppress EMT in breast cancer, while it can induce EMT in prostate cancer[24,28,29]. Since HL156A

can inhibit the SIRT1 expression, cell migration, and cell invasion, we suspect that the EMT process might be targeted too; therefore, we decided to check the EMT markers to confirm our hypothesis. As demonstrated in figure 3, treatment of HL156A at the IC50 concentration (40 μM) inhibits both epithelial and mesenchymal markers. At the lower dose (20 μM), 24-hours treatment of HL156A possibly reverts the EMT process, as the epithelial markers E-cadherin, β-catenin, and Claudin are upregulated while the mesenchymal markers N-cadherin, Vimentin, and Slug are downregulated. Further studies need to be conducted to elucidate the potential of HL156A as an EMT regulator.

Literature reported that metformin can regulate autophagy in cancer[9,18]. Because metformin is the precursor of HL156A, we decided to test whether HL156A can induce autophagy in OSCC. As demonstrated in Figure 4 and Figure 9, 24 hours treatment of HL156A induces autophagy in all three OSCC cell lines, as the LC3B expression, LC3B-positive structures are induced. To further verify the induction of autophagy, we stained the lysosome and autophagic vacuoles through AO and MDC staining, which both yielded a positive result and confirmed that HL156A can induce autophagy in OSCC cell lines.

The role of autophagy in cancer is complicated, and there is a growing body of studies suggest that inhibition of autophagy is a potential approach to increase the effectiveness of cancer therapy[30].The most common strategy is to target the late stage of autophagy - the fusion step using either Chloroquine (CQ), Hydroxychloroquine (HCQ), or newly synthesized drugs DQ661 or Lys05 [30]. Therefore, we decided to inhibit the HL156A-induced autophagy by CQ, through the co-treatment method. As illustrated in Figure 5-7, the combination of HL156A and CQ exhibits a greater anti-cancer effect than

HL156A treatment alone, suggesting that the HL156A-induced autophagy reveals a protective role. Inhibition of CQ further boosts the HL156A-induced cell apoptosis, as indicated with the higher reduction in the protein level of inactivating form of PARP-1 and Caspase-3. We also conducted in vivo experiment on nude mice model to further validate the synergize between HL156A and CQ. Tumor sizes were significantly reduced in the co-treated group compared with the single treatment group. Moreover, HE staining showed an increase in apoptotic and/or necrotic cells with a large amount of nuclear fragmentation.

Overall, this is the first-time reports that HL156A induces autophagy-protective besides the anti-proliferation effect on the oral cancer cell. Using combination HL156A and autophagy inhibitor chloroquine has a synergic effect against tumor cancer cells in both in *vitro* and in *vivo* experiments. These findings indicate that an HL156A and Chloroquine combination treatment may be a potential therapeutic regimen for cancer treatment. Results from our study can stimulate further interest in the key and role of SIRT 1 in the oral cancer cell; it might be a potential target for epithelial-mesenchymal transition in the oral cancer cell.

Figure 10

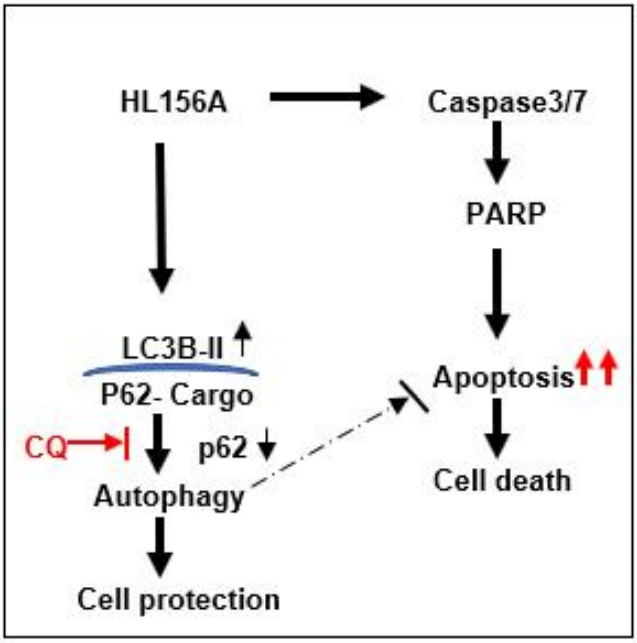

Figure 10. Schematic diagram of the mechanism of HL156A-mediated autophagy attenuation of apoptosis which stimulates by HL156A in oral squamous cell carcinoma.

V. REFERENCES

1. Mendenhall WM, Foote RL, Sandow PR, Fernandes RP. Chapter 30 - Oral Cavity Cancer. In: Gunderson LL, Tepper JEBT-CRO (Third E, eds. W.B. Saunders; 2012:553-583. doi:https://doi.org/10.1016/B978-1-4377-1637-5.00030-4

2. Farooq I, Bugshan A. Oral squamous cell carcinoma: Metastasis, potentially associated malignant disorders, etiology and recent advancements in diagnosis. F1000Research. 2020;9:1-10. doi:10.12688/f1000research.22941.1

3. Rha SY, Beom S-H, Shin YG, et al. Phase I study of IM156, a novel potent biguanide oxidative phosphorylation (OXPHOS) inhibitor, in patients with advanced solid tumors. J Clin Oncol. 2020;38(15_suppl):3590. doi:10.1200/JCO.2020.38.15_suppl.3590

4. Foretz M, Guigas B, Viollet B. Understanding the glucoregulatory mechanisms of metformin in type 2 diabetes mellitus. Nat Rev Endocrinol. 2019;15(10):569-589. doi:10.1038/s41574-019-0242-2

5. Ugwueze C V., Ogamba OJ, Young EE, Onyenekwe BM, Ezeokpo BC. Metformin: A Possible Option in Cancer Chemotherapy. Anal Cell Pathol. 2020;2020. doi:10.1155/2020/7180923

6. Aljofan M, Riethmacher D. Anticancer activity of metformin: A systematic review of the literature. Futur Sci OA. 2019;5(8). doi:10.2144/fsoa-2019-0053

7. Vancura A, Bu P, Bhagwat M, Zeng J, Vancurova I. Metformin as an Anticancer Agent. Trends Pharmacol Sci. 2018;39(10):867-878. doi:10.1016/j.tips.2018.07.006

8. Zheng Z, Bian Y, Zhang Y, Ren G, Li G. Metformin activates AMPK/SIRT1/NF-κB pathway and induces mitochondrial dysfunction to drive caspase3/GSDME-mediated cancer cell pyroptosis. Cell Cycle. 2020;19(10):1089-1104. doi:10.1080/15384101.2020.1743911

9. Gao C, Fang L, Zhang H, Zhang WS, Li XO, Du SY. Metformin induces autophagy via the ampk-mtor signaling pathway in human hepatocellular carcinoma cells. Cancer Manag Res. 2020;12:5803-5811. doi:10.2147/CMAR.S257966

10. Choi J, Lee JH, Koh I, et al. Inhibiting stemness and invasive properties of glioblastoma tumorsphere by combined treatment with temozolomide and a newly designed biguanide (HL156A). Oncotarget. 2016;7(40):65643-65659. doi:10.18632/oncotarget.11595

11. Kim SA, Lam TG, Yook JI, Ahn SG. Antioxidant modifications induced by the new metformin derivative HL156A regulate metabolic reprogramming in SAMP1/kl (-/-) mice. Aging (Albany NY). 2018;10(9):2338-2355. doi:10.18632/aging.101549

12. Jeong YS, Lam TG, Jeong S, Ahn SG. Metformin derivative hl156a reverses multidrug resistance by inhibiting hoxc6/erk1/2 signaling in multidrug-resistant human cancer cells. Pharmaceuticals. 2020;13(9):1-15. doi:10.3390/ph13090218

13. Lam TG, Jeong YS, Kim SA, Ahn SG. New metformin derivative HL156A prevents oral cancer progression by inhibiting the insulin-like growth factor/AKT/mammalian target of rapamycin pathways. Cancer Sci. 2018;109(3):699-709. doi:10.1111/cas.13482

14. Tsogbadrakh B, Ju KD, Lee J, et al. HL156A, a novel pharmacological agent with potent adenosine-monophosphate-activated protein kinase (AMPK) activator activity ameliorates renal fibrosis in a rat unilateral ureteral obstruction model. PLoS One. 2018;13(8):1-15. doi:10.1371/journal.pone.0201692

15. Chun Y, Kim J. Autophagy: An Essential Degradation Program for Cellular Homeostasis and Life. Cells. 2018;7(12):278. doi:10.3390/cells7120278

16. Xiao Z, Gaertner S, Morresi-Hauf A, et al. Metformin Triggers Autophagy to Attenuate Drug-Induced Apoptosis in NSCLC Cells, with Minor Effects on Tumors of Diabetic Patients. Neoplasia. 2017;19(5):385-395. doi:https://doi.org/10.1016/j.neo.2017.02.011

17. De Santi M, Baldelli G, Diotallevi A, Galluzzi L, Schiavano GF, Brandi G. Metformin prevents cell tumorigenesis through autophagy-related cell death. Sci Rep. 2019;9(1):1-11. doi:10.1038/s41598-018-37247-6

18. De Santi M, Baldelli G, Diotallevi A, Galluzzi L, Schiavano GF, Brandi G. Metformin prevents cell tumorigenesis through autophagy-related cell death. Sci Rep. 2019;9(1):1-11. doi:10.1038/s41598-018-37247-6

19. Choi H. HL156 compounds , novel metformin derivatives , inhibit angiogenesis through AMPK mediated downregulation of FOXM1 in gastric cancer cells HL156 compounds , novel metformin derivatives , inhibit angiogenesis through AMPK mediated downregulation of FOXM1 i.

20. Cuyàs E, Verdura S, Llorach-Parés L, et al. Metformin Is a Direct SIRT1-Activating Compound: Computational Modeling and Experimental Validation . Front Endocrinol . 2018;9:657. https://www.frontiersin.org/article/10.3389/fendo.2018.00657

21. Kim H-W, Kim S, Ahn S-G. Sirtuin inhibitors, EX527 and AGK2, suppress cell migration by inhibiting HSF1 protein stability. Oncol Rep. 2015;35. doi:10.3892/or.2015.4381

22. Ren Z, He H, Zuo Z, Xu Z, Wei Z, Deng J. The role of different SIRT1-mediated signaling pathways in toxic injury. Cell Mol Biol Lett. 2019;24(1):1-10. doi:10.1186/s11658-019-0158-9

23. Michan S, Sinclair D. Sirtuins in mammals: Insights into their biological function. Biochem J. 2007;404(1):1-13. doi:10.1042/BJ20070140

24. Shi L, Tang X, Qian M, et al. A SIRT1-centered circuitry regulates breast cancer stemness and metastasis. Oncogene. 2018;37(49):6299-6315. doi:10.1038/s41388-018-0370-5

25. Kupis W, Pałyga J, Tomal E, Niewiadomska E. The role of sirtuins in cellular homeostasis. J Physiol Biochem. 2016;72(3):371-380. doi:10.1007/s13105-016-0492-6

26. Haigis MC, Guarente LP. Mammalian sirtuins - Emerging roles in physiology, aging, and calorie restriction. Genes Dev. 2006;20(21):2913-2921. doi:10.1101/gad.1467506

27. Islam S, Abiko Y, Uehara O, Chiba I. Sirtuin 1 and oral cancer (Review). Oncol Lett. 2019;17(1):729-738. doi:10.3892/ol.2018.9722

28. Byles V, Zhu L, Lovaas JD, et al. SIRT1 induces EMT by cooperating with EMT transcription factors and enhances prostate cancer cell migration and metastasis. Oncogene. 2012;31(43):4619-4629. doi:10.1038/onc.2011.612

29. Nogueiras R, Habegger KM, Chaudhary N, et al. NIH Public Access. 2013;92(3):1479-1514. doi:10.1152/physrev.00022.2011.SIRTUIN

30. Marta P, Arias A, Mart D, Ricardo P, Quesada R, Soto-cerrato V. Targeting autophagy for cancer treatment and tumor chemosensitization.Cancers 2019, 11, 1599; doi:10.3390/cancers11101599

Ⅵ. 국문 초록

구강 편평 세포 암종에서 메트포르민 유도체 HL156A 유도 세포 사멸과 자가 포식 사이의 새로운 연관성

NGUYEN MANH TUONG
지도교수: 안상건
조선대학교 대학원
치의생명공학과

항 당뇨 치료제 인 메트포르민은 구강 편평 세포 암종 (OSCC)을 포함한 많은 암에서 항 종양 효과를 발휘한다. 이러한 최근의 발전에도 불구하고 근본적인 분자 메커니즘은 명확하게 밝혀지지 않았다. 흥미롭게도, 우리의 최근 연구는 메트포민 유도체 HL156A가 다른 구강암 세포의 성장을 억제 할 수 있다고 보고했다. 본연구에서는 구강암 세포에서 HL156A의 항 증식 역할과 작용 기전을 조사하였다. MTT 및 콜로니 형성 분석을 사용하여 HL156A가 농도 의존적으로 발생한 구강암 세포에서 항 증식 효과가 있음을 발견하였다. 유세포 분석을 사용하여 세포주기 및 세포 사멸을 분석하였고, HL156A에 대한 노출은 G2 / M 단계에서 세포주기 정지를 유도하고 세포 apoptosis를 증가시켰다. 이는 증가 된 caspase3 / PARP 활성과 관련이 있다. 다른 한편으로, HL156A는 또한, autophagic vacuoles을 염색하는 acridine orange염색 및 자가 리소좀 관련 LC3 단백질의 정량화에 의해 확인된 바와 같이 자가 포식을 유도했다. 흥미롭게도, autophagy 억제제 chloroquine (CQ)에 의한 autophagy의 억제는 apoptosis를 증가시키고 구강암 세포에서 HL156A의 anti proliferation 효과를 촉진하여 autophagy가 HL156A에 의한 apoptosis를 억제한다. 이러한 관찰의 관련성은 HL156A 및 CQ 처리와의 공동 처리가 구강암 세포 이종 이식 마우스에서 종양 성장을 강력하게 억제한다는 것을 보여 주었기 때문에 생체 내 시스템에서 확인되었다. 이러한 결과는 HL156A가 세포주기 정지 및 세포 사멸과 관련된 항 증식 효과가있는 반면, 세포 보호를 위해 자가 포식을 유도함을 보여 주었다. 종합하여, 우리는 HL156A의 anti proliferation 효과와 구강암 세포에서의 치료 접근법에 대한 새로운 기계론적 통찰력을 증명했습니다.